Publishing House
A K A P I T

COMPUTER METHODS IN MATERIALS SCIENCE
Informatyka w Technologii Materiałów

Vol. 18, 2018, No. 4

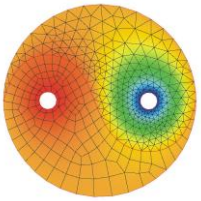

USING NEURAL NETWORKS TO PREDICT THE FLOW CURVES AND PROCESSING MAPS OF TNM-B1

JOHAN ANDREAS STENDAL*, ALIAKBAR EMDADI, IRINA SIZOVA, MARKUS BAMBACH

[1]Panta Rhei Gebäude, Konrad-Wachsmann-Allee 17, 03046 Cottbus, Germany
[*]Corresponding author: Stendal@b-tu.de

Abstract

The ability to predict the behavior of a material is vital in both science and engineering. Traditionally, this task has been carried out using physics-based mathematical modeling. However, material behavior is dependent on a wide range of interconnected phenomena, properties and conditions. During deformation processes, work hardening, softening, microstructure evolution and generation of heat all occur simultaneously, and can either cooperate or compete. In addition, they can vary with the deformation temperature, applied force and process speed. As the complete picture of material behavior from the macroscopic scale to the atomic scale is not yet fully understood, deformation processes such as hot forging can be difficult to handle using physics-based modeling. Usually, modeling the high temperature deformation behavior of metals consists of extracting characteristic points from the experimental flow curve data, and use them to fit the model equations through regression analysis. This is called phenomenological modeling, as it is based on the observations of a phenomena rather than being derived from fundamental theory. Alternatively, the data obtained from experiments could be used for a data-driven or machine learning (ML) approach to model the material behavior. An ML model would require no knowledge of the underlying physical phenomena governing a deformation process, as it can learn a mapping function which connects input to output based purely on the experimental data. In this work, the application of machine learning to modeling the flow curves of two different states of the titanium aluminide (TiAl) TNM-B1; hot isostatically pressed (HIPed) and heat treated, is investigated. Neural networks were used to learn a mapping function which predicted flow stress based on the inputs temperature, strain and strain rate. In addition, strain rate sensitivity maps and processing maps based on the experimental and the predicted data are analysed and compared. The results revealed that the neural networks were able to produce realistic and accurate flow curves, which fitted to the underlying behavior of the experimental data rather than the noise. The strain rate sensitivity and processing maps showed conflicting results. Good correlation was found for the HIPed material state between the ones based on experimental data and the ones based on predicted values, while there was a significant difference for the heat treated state.

Key words: Machine learning, Processing maps, Titanium aluminide, TNM-B1

1. INTRODUCTION

Machine learning has made many contributions to society in the past decade. Self-driving cars, speech recognition, internet search recommendations and computers beating humans at board games are all the results of the continual improvements to computational power and learning algorithms. In material science, models based on machine learning may be promising due to the abundance of experimental data in the field. ML has already been implemented to enhance and accelerate several areas of research. These include the prediction of material behavior and properties, and the discovery of new and useful materials based on existing databases and experimental data, such as stress-strain data and chemical composition data (Pilania et al., 2013; Liu et al., 2017). Notably, previous studies have explored the application of pure machine learning as well as hybrid approaches to material modeling. Lin et al. (2008) developed an artificial neural network (ANN) model to predict the flow stress behavior of a 42CrMo steel during hot compression. The ANNs were trained on temperature, strain and strain rate

data to learn a mapping function that could output flow stress. The authors used the performance indicator average absolute relative error (AARE), and achieved a value of around 4.5 % when testing the ANN on new data not used for training the network. Zhu et al. (2003) developed a hybrid model consisting of a combination of neuro-fuzzy and physical-based models. The aim was to predict flow stress and microstructure evolution during thermomechanical processing of aluminium-magnesium alloys. The hybrid model was integrated into a finite element simulation, which gave very similar results as compared to empirical models. Yu et al. (2010) used a fuzzy neural network (FNN) in order to predict ultimate tensile strength, yield strength, elongation and area reduction of Ti-6Al-4V based on forging temperature, strain and strain rate. An FNN uses a neural network to find the parameters of a fuzzy rule set. It was verified that the model can predict the mechanical properties, which can aid in practical optimization of processing parameters. Sheikh et al. (2008) employed two parallel ANN models to predict the flow stress of a 5083 aluminium alloy, in regions of serrated flow and smooth yielding respectively, during tensile testing at room temperature and elevated temperatures. The experimental temperature, strain and strain rate data were used as training inputs to learn a mapping function which outputs flow stress. The results showed good agreement between the experimental data and predicted values for both warm and cold conditions. Prasad & Seshacharyulu (1998) investigated the use of processing maps for different titanium alloys to design hot working processes.

This work focuses on the titanium aluminide (TiAl) TNM-B1), an attractive material to the aerospace, automotive, power generation and related industries due to its strength to weight ratio, high resistance to heat, corrosion and creep. To study metal forming processes such as hot forging, finite element (FE) simulations are widely used, and their reliability is largely determined by the accuracy of the material model applied. For TiAl alloys, the material models describing hot deformation behavior are empirical and phenomenological models that were originally derived for steels and adapted to TiAl (Cheng et al., 2014). As steel is generally hot worked in the austenitic phase, these models were designed for a single phase material. Although models for TiAl have exhibited high accuracy, they do not account for the reorientation of lamellar colonies, flow localization, and the deformation behavior of the individual phases, which strongly influence the deformation behavior of TiAl alloys (Cingara & McQueen, 1992; Bambach et al., 2016). There is a knowledge gap in understanding the behavior of TiAl alloys during deformation processes, due to their multi-phase nature and complicated microstructural features. Additionally, microstructural phenomena such as dynamic recrystallization (DRX), dynamic recovery (DRV) and the rotation of lamellar colonies heavily influence the deformation behavior (Inui et al., 1995). This study aims to develop and explore the performance of a pure machine learning model to learn the course of the flow curves for hot isostatic pressed (HIPed) and heat treated TNM-B1. In addition, the correlation between processing maps and strain rate sensitivity maps based on the experimental and predicted data was investigated. Hot compression tests of the TNM-B1 material were performed to extract experimental flow stress data. The tests were conducted at the temperatures 1150, 1175 and 1200°C, and the strain rate 0.005 s^{-1}.

2. MATERIAL AND METHODS

2.1. Material and microscopy

The TNM-B1 material with a composition given in table 1 was produced using a vacuum arc remelting (VAR) method at GfE Metalle und Materialien GmbH (Germany). The material was then hot isostatic pressed (HIPed) to close microporosities, using the parameters 1200 °C, 200 MPa and 4 h. The produced ingot had a height of 150 mm and a diameter of 49 mm. The finished ingot was then eroded into cylinders with a height of 95 mm and a diameter of 7 mm, using electrical discharge machining (EDM) by Erocontur GmbH (Germany). The cylinders were cut and turned into test samples with a height of 8 mm and a diameter of 5 mm.

Table 1. Chemical composition of alloy TNM-B1 as certified by GfE.

	Ti	Al	Nb	Mo	B	O	Fe	Ni	C	Cr	Si	N	H	Cu	Y
at.%	bal	43.7	4.0	1.0	0.1	-	-	-	-	-	-	-	-	-	
wt%	bal	28.65	9.15	2.36	0.026	0.063	0.037	0.012	0.011	0.009	0.008	0.003	0.002	0.001	0.001

To investigate the microstructure of the samples a TESCAN Mira II (Czech Republic) scanning electron microscope (SEM) was used. All images were made in back-scattered electron (BSE) mode with an acceleration voltage of 14,5 kV. Prior to imaging, the sample surface was grinded with a RotoPol-22 from Struers (Germany), using a speed of 300 rpm and a force of 20 N. SiC grinding paper with a gradation ranging from 240 to 2500 was used. After grinding, the samples were polished for 72 hours in a VibroMet 2 from Buehler (Switzerland). The samples were suspended in distilled water and Collodial Silica, from the LECO Corporation (USA).

2.2. Compression tests and heat treatment

A DIL805A/D/T quenching and deformation dilatometer from Bähr Thermoanalyse (Germany) was used to perform the compression tests. Molybdenum plates with a thickness of around 1 mm were placed between the specimen and the Si3N4-punches in the dilatometer, and an argon protective atmosphere was used to protect the samples from oxidation. The cylindrical samples were isothermally deformed using the following parameters; strain ranging from 0 to 0.8, a constant strain rate of 0.005 s^{-1} and temperatures 1150°C, 1175°C and 1200°C. The samples and molybdenum plates were first heated by induction at a heating rate of 10 K/s, and held at the testing temperature for 3 minutes. This was done to obtain a homogeneous microstructure and quasi-isothermal conditions before deformation. The samples were then deformed to a strain of 0.8. Finally, the samples were cooled using argon gas with a cooling rate of 200 K/s. The experiments were duplicated at least two times to ensure repeatability of the flow curves.

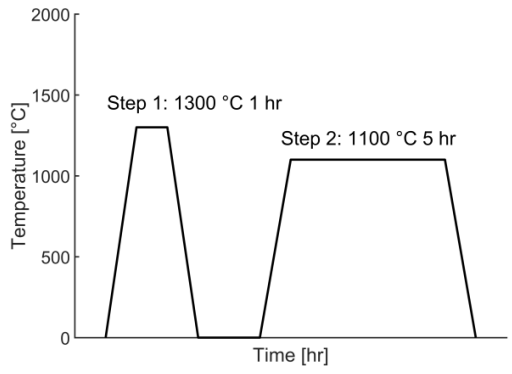

Fig. 1. *Heat treatment procedure.*

The heat treatment procedure used in this work is illustrated in figure 1. It was performed in two steps in a furnace from Nabertherm GmbH (Germany). In the first step, the samples were held at 1300°C for 1 hour. In the second step, the samples were held at 1100°C for 5 hours. After each step, the samples were air-cooled.

2.3. Neural network fundamentals

The machine learning model used an artificial neural network as its framework (figure 2). Based on the principle of supervised learning, where both the training inputs and the intended output are known variables, an algorithm was used to learn a mapping function between the two. Artificial neural networks are inspired by the biological neural networks that comprises our brains, and attempts to replicate the way we humans learn and process information (Anderson, 1995). They consist of interconnected artificial neurons or processing elements organized in layers; an input layer, an output layer, and hidden layers in between. The ANN is referred to as shallow if it has one hidden layer and deep (i.e. deep learning) if the number of hidden layers exceeds one. The aim was to train a learning algorithm to predict flow stress during hot deformation of TNM-B1 as a function of temperature, strain rate and strain. For more in-depth reading regarding artificial neural networks, see Rojas (1996).

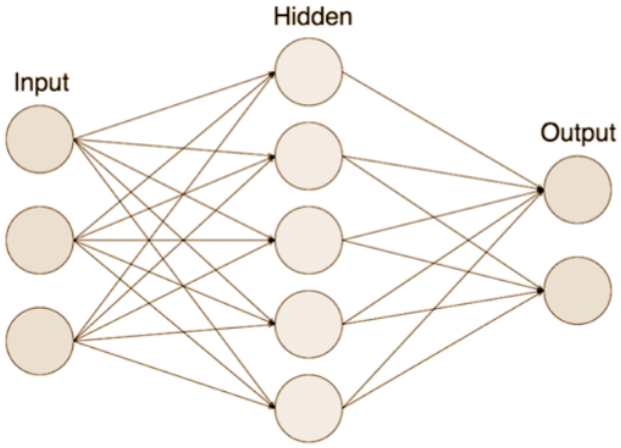

Fig. 2. *Neural network schematic.*

Each layer of the ANN consists of a number of artificial neurons. Simply put, an artificial neuron receives inputs from other nodes in an earlier hidden layer or from the original input data, and computes an output. It does this by calculating a weighted sum of its inputs and adding a bias, where the weights and the biases are parameters to be learned. An activation function is then applied to decide if the neu-

ron should fire or not fire (i.e. pass along its output to other neurons). The following equation describes how the inputs are weighted and summed and how the bias is added:

$$f(x) = \sum(w_i x_i) + b \quad (1)$$

where: x_i - the inputs, w_i - the weights, b - the bias.

This sum is then passed through a sigmoid activation function, which translates the sum to a single output between 0 and 1. If this final output is above a certain threshold, the neuron fires. The purpose of the activation function is to introduce non-linearity to the neuron output, as most real world data is non-linear. This process of passing the input data through the neurons of the neural network is called feed forward. After one feed forward, the resulting output of the network is compared to the known intended output via a cost function. In this work, the mean squared error (MSE) cost function was used:

$$MSE = \frac{1}{n}\sum_{i=1}^{n}\left(Y_i - \hat{Y}_1\right)^2 \quad (2)$$

where: Y_i - the known intended output, $\hat{Y}_1$ - the predictions made by the neural network, n - the number of data points.

An optimization function then attempts to minimize this cost in order to improve the performance of the ANN (i.e. making predictions closer to the intended output). It does this by going backwards through the ANN and manipulating the weights and biases in a process called back propagation. One cycle of feed forward and back propagation is called an epoch. In theory, each completed epoch will increase the network performance, until diminishing returns, overfitting (i.e. fitting the noise in the input data) or even increases in the cost function occurs. The Levenberg–Marquardt optimization algorithm was used in this work, a widely used non-linear least squares fitting algorithm first proposed by Kenneth Levenberg and later improved by Donald Marquardt (Levenberg, 1944; Marquardt, 1963).

2.4 Processing- and strain rate sensitivity maps fundamentals

The main goal of these maps is to predict the optimal hot forging conditions and the instability regions of TNM-B1. The construction of processing maps is based on the principles of dynamic material modeling, and consists of superimposing a power dissipation efficiency map and an instability parameter map at a constant strain (Prasad & Sasidhara, 1997). In short, the workpiece is considered a full dissipater of the total power input during hot deformation. The power (P) is divided into two parts; one is the energy dissipated as heat generation (G), and the other is energy dissipated due to microstructure evolution (J), as given by equation:

$$P = G + J = \int_0^{\dot{\varepsilon}} \sigma d\dot{\varepsilon} + \int_0^{\sigma} \dot{\varepsilon} d\sigma = \sigma\dot{\varepsilon} \quad (3)$$

The efficiency of power dissipation (η) is given by:

$$\eta = \frac{J}{J_{\max}} = \frac{2m}{m+1} \quad (4)$$

The criterion for metallurgical instability and the instability parameter (ξ) is calculated as:

$$\frac{dJ}{d\dot{\varepsilon}} < \frac{J}{\dot{\varepsilon}} \rightarrow \xi = \frac{\partial \ln\left(\frac{m}{m+1}\right)}{\partial \dot{\varepsilon}} + m < 0 \quad (5)$$

In equations (4) and (5) m is the strain rate sensitivity parameter in the constitutive equation for flow stress at a constant temperature and strain:

$$\sigma = K\dot{\varepsilon}^m \quad (6)$$

Variation of (η) with temperature and strain rate while keeping strain constant constitutes the power dissipation map. Variation of (ξ) with temperature and strain rate while keeping strain constant constitutes the instability map. The superposition of these two maps constitutes the processing map.

3. RESULTS AND DISCUSSION

3.1. Microstructure and deformation overview

The hot deformation of the HIPed and heat treated TNM-B1 samples led to a microstructure consisting of lamellar colonies, cellular and globular structures with varying grain sizes, as displayed in figure 3. The loading direction is along the y-axis. TNM-B1 consist of the ordered phases γ-TiAl (dark contrast), α_2–Ti_3Al (gray contrast) and β_0–TiAl (bright contrast). The phases all have different individual deformation behaviors (Schloffer et al., 2012; Masahashi et al., 1991). The α-phase has a hexagonal close-packed (HCP) D structure, and has the highest strength and lowest deformability in the TNM-B1 system. The γ-phase has a face-centered cubic (FCC) L10 crystal structure. It has higher strength than the β-phase, but higher deformability than the α-phase.

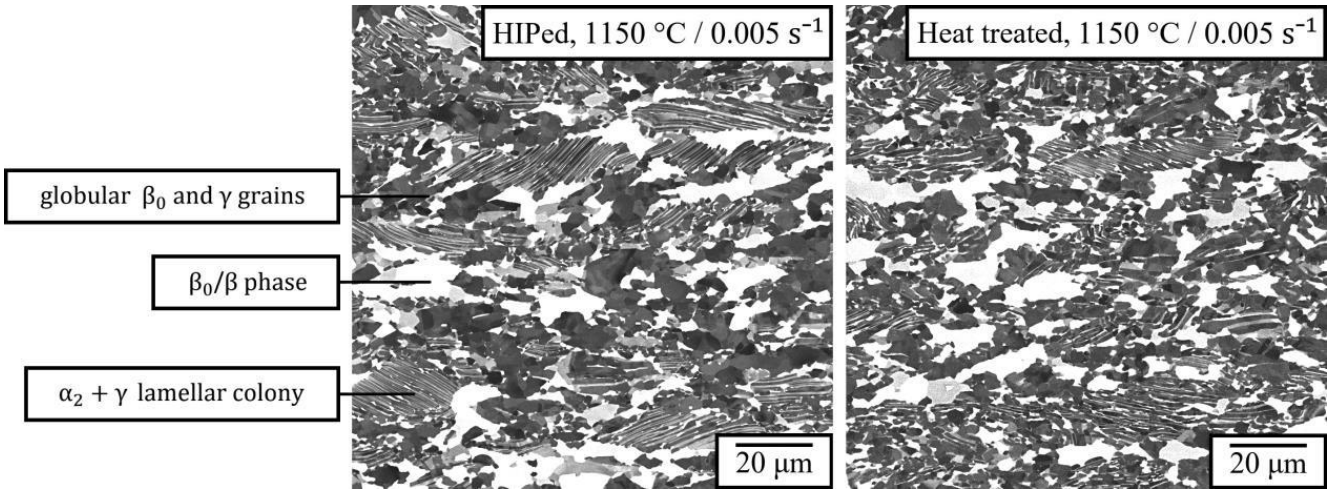

Fig. 3. *Electrical contact rivets: (a) solid - silver, (b) bimetallic – silver / copper, (c) cross-section of assembled bimetallic electric contact.*

The β-phase has a body-centered cubic (BCC) B2 structure. At high temperatures, it is the softest phase in the TNM-B1 system (Liu et al., 2015). Therefore, the *β*-phase carries a much higher strain during hot deformation than the nominal value, leading to highly misoriented subgrains and dynamic recrystallization (DRX). In general, themacroscopic deformation behavior of TNM-B1 depends strongly on DRX, dynamic recovery (DRV) and the orientation and deformation of lamellar colonies

3.2. Flow curves

An artificial neural network was trained on the experimental flow curve data for TNM-B1. It learned through the experimental examples a mapping function which uses temperature, strain and strain rate to make predictions on the flow stress values. First, the dataset was cleaned. To reduce overfitting to small variations in temperature and strain rate and promote fitting between strain and stress, the temperature and strain rate vectors data vectors were converted to constant values. The final dataset used for training the neural network consisted of constant temperature and strain rate values, and the original experimental strain and stress data. A split of 70% training data, 15 % test data and 15% validation data was used. Through a process of trial and error the optimal neural network parameters for this particular case was found. This was done by iteratively tuning the number of layers and neuron in the network and evaluating the predictive performance. The optimal architecture found was 2 hidden layers with 10 neurons in the first layer and 3 in the second. The neural network with the best performance achieved an MSE (mean squared error) of 6.7 (equivalent to an average error in MPa of around 2.6). In all, 25 824 training examples were used from 6 different flow curves, 2 for each condition. The predicted flow curves for the HIPed state of TNM-B1 along with the experimental results are displayed in figure 4.

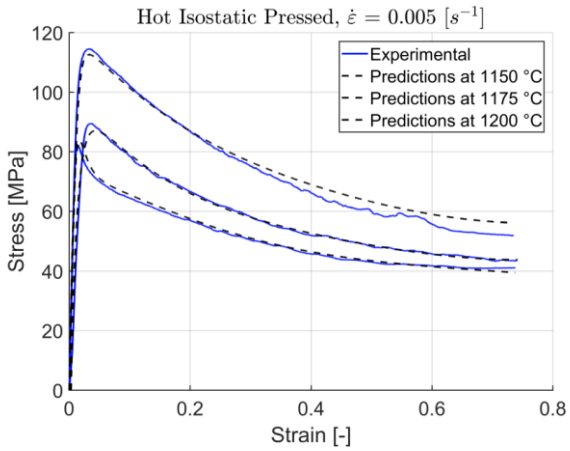

Fig. 4. *Experimental and predicted flow curves for HIPed TNM-B1, obtained at a strain rate of 0.005 s^{-1} and the temperatures 1150, 1175 and 1200°C.*

The experimental flow curves of TNM-B1 show an initial steep rise in stress up to a pronounced peak, followed by a strong softening behavior, mainly due to DRX, until a steady-state is reached. As is evident from the results, the neural network was able to reproduce the shape of the flow curve almost exactly from the experimental data. Generating the network took around 2 min., and the computing time after training was in the order of 0.01 s. The ma-

chine learning model was able to produce very accurate predictions and highly realistic flow curves, purely based on experimental data. The learning algorithm was able to capture the characteristic distinct features of the TNM-B1 flow curves, such as the sharp peak and the strong softening behaviour, without fitting to the unwanted noise in the data. This indicates that the generated neural network was not overly complex, and was fitted to the underlying behaviour of the data instead of the noise in the data. The results indicates that the equations comprising traditional physics-based models can be replaced by a mapping function generated by a neural network. However, as with traditional models, problems can arise when interpolating or extrapolating results. Neural networks are known to be able to interpolate between inputs used for training, while extrapolating can be problematic. This approach can seemingly be applied to any material, however the need for experimental data to develop both traditional and machine learning models remains constant.

Figure 5 displays the experimental and predicted flow curves for the heat treated state of TNM-B1. The same procedure and network architecture was applied on the experimental data for the heat treated material state and the HIPed state. The neural network with the best performance achieved an MSE (mean squared error) of 8.6 (equivalent to an average error in MPa of around 2.9). In all, 25 824 training examples were used from 6 different flow curves, 2 for each condition. Generating the network took around 1.5 minutes, and the computing time after training was in the order of 0.01 s. Again, the machine learning model was able to produce accurate predictions based only on experimental data. There was a higher variance for the same conditions in the experimental results of the heat treated state than the HIPed state. However, the results reveal that the neural network was able to predict generalized flow curves, which did not fit to data far removed from the mean. This can specifically be seen in the results at 1150°C and at 1200°C after around 0.4 strain. This indicates that the developed neural network was able to give realistic predictions even with inconsistent experimental data. An interesting topic for future research can be investigating the possibility of interpolating between heat treatment states of a material (e.g. a titanium aluminide alloys) using machine learning. This could be done by including microscopy image data (e.g. SEM pictures) in training the machine learning model, to predict flow curves that are also based on the microstructures of different material states. However, copious amounts of experimental data is potentially required for training such a model.

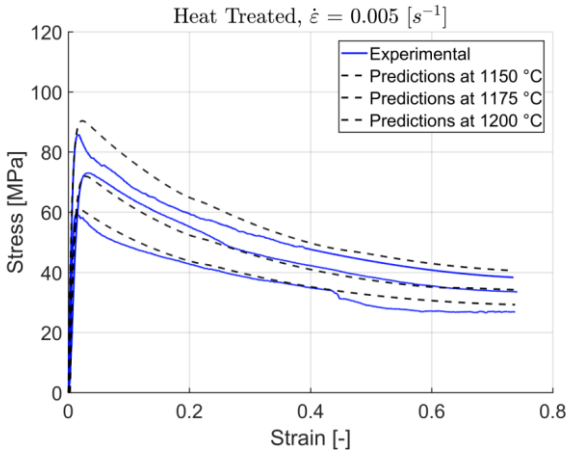

Fig. 5. *Experimental and predicted flow curves for heat treated TNM-B1, obtained at a strain rate of 0.005 s^{-1} and the temperatures 1150, 1175 and 1200°C.*

3.3. Processing- and strain rate sensitivity maps

Figures 6 and 7 display the processing maps and strain rate sensitivity maps for HIPed and heat treated TNM-B1 respectively, generated from both the experimental and predicted flow curve data obtained at 0.5 strain.

There is no exact match between the maps based on the experimental data and the maps based on the predicted values. Positive m values are observed for all conditions for the experimental HIPed state (figure 6a) and the predicted HIPed state (figure 6c). Negative ^{m} values (marked in gray) can be seen for the experimental heat treated state (figure 6a) at the conditions 1200°C/0.0013 s^{-1} and 1200°C/0.05 s^{-1}, indicating that no restoration mechanisms (e.g. DRX and DRV) are active in the regions, while the predicted heat treated state (figure 7c) shows negative m values at the conditions 1150°C/0.0013 s^{-1} and 1150°C/0.05 s^{-1}. Flow instability regions (marked in gray) in both the experimental HIPed state (figure 6b) and the predicted HIPed state (figure 6d) are observed at the conditions 1150°C/0.005 s^{-1}. Flow instability is also observed at the conditions 1200°C/0.05 s^{-1} for the experimental HIPed state and 1200°C/0.005 s^{-1} for the predicted HIPed state. For the heat treated state (figures 7b and 7d), the flow instability regions are observed at the conditions 1165°C/0.05 s^{-1} and 1200°C/0.0013 s^{-1} based on the experimental data, and at 1150°C/0.0013 s^{-1} and 1180°C/0.05 s^{-1} based on the predicted data.

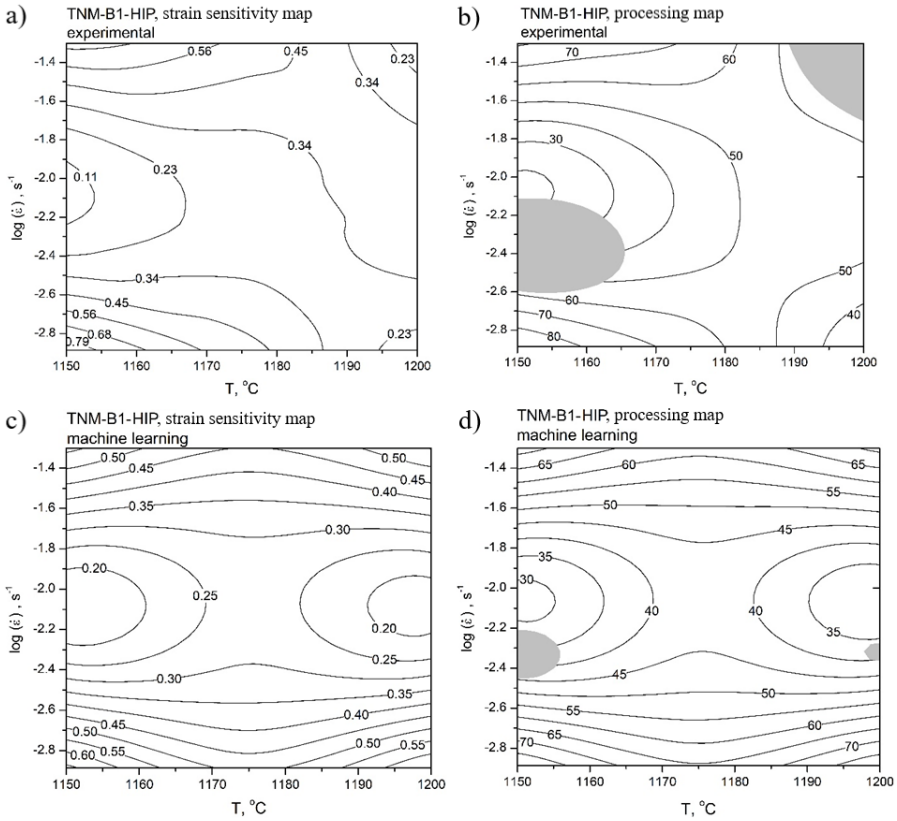

Fig. 6. *Strain rate sensitivity maps for the experimental (a) and machine learning (c) results. Processing maps for the experimental (b) and machine learning (d). All generated from the experimental and predicted data of HIPed TNM-B1, at a strain of 0.5.*

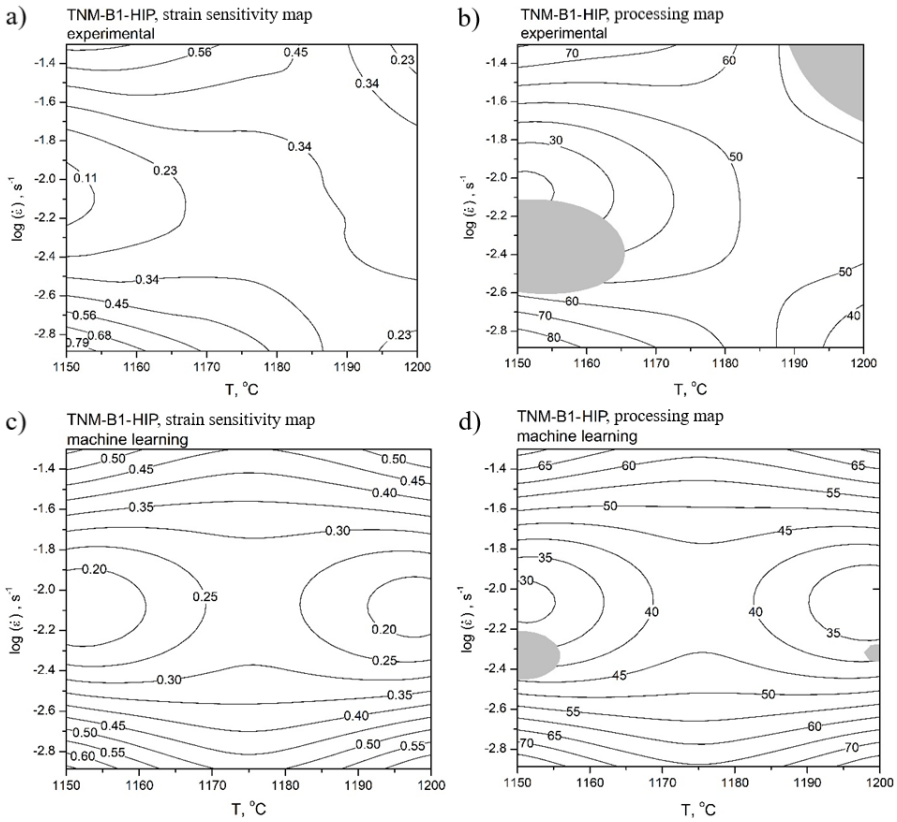

Fig. 7. *Strain rate sensitivity maps for the experimental (a) and machine learning (c) results. Processing maps for the experimental (b) and machine learning (d). All generated from the experimental and predicted data of HIPed TNM-B1, at a strain of 0.5.*

The optimal processing conditions is found where the highest *m* value without flow instability. This is observed to be around 1150°C/0.0013 s^{-1} for the HIPed state, based both on the experimental and predicted data. The optimal conditions for the heat treated state is observed to be around 1170°C/0.005 s^{-1} based on the experimental data, and around 1160°C/0.005 s^{-1} based on the predicted data. The strain sensitivity maps and the processing maps based on the predicted data for the HIPed material state show partial correlation and predict the same optimal processing conditions. For the heat treated state, only a slight correlation between the maps based on experimental and predicted data can be observed, and there is a mismatch between the suggested optimal conditions. The results are conflicting, as the maps for the HIPed state correlate sufficiently to give the same optimal processing conditions, while there was a significant difference in the maps based on experimental and predicted data for the heat treated state. This is likely due to the higher variance in the compression test data for the heat treated state, as this caused a bigger difference in experimental and predicted flow stresses. Further research in this area can include a damage behaviour analysis to verify the maps and the optimal processing conditions

4. CONCLUSIONS

This study has explored utilizing neural networks to predict the course of the flow curves of two material states of the titanium aluminide alloy TNM-B1; hot isostatically pressed (HIPed) and a heat treated state. The neural networks were trained on experimental flow stress data examples to predict flow stress as a function of temperature, strain and strain rate. For this purpose, hot compression tests of the TNM-B1 material were performed at the temperatures 1150, 1175 and 1200°C, and a strain rate of 0.005 s^{-1}. In addition, the correlation between strain rate sensitivity maps and processing maps based on experimental and predicted data was investigated. It appears that machine learning models are not readily capable to generate outputs such as processing maps, and future research is needed. One possibility can be to directly learn to generate both the flow curves and processing maps using separate neural networks, so that future calculations based on the processing maps are possible without information loss. In addition, future work can include investigating the use of microstructural data (e.g. SEM images) to predict flow curves and to interpolate between material states, and to investigate damage behavior to evaluate and verify the strain rate sensitivity maps and processing maps.

The main conclusions drawn from this investigation are:

- Based purely on experimental data, neural networks which could accurately and realistically predict the flow curves of both HIPed and heat treated TNM-B1 were developed. The achieved average stress errors in MPa were 2.6 and 2.9 for the HIPed and heat treated state respectively.
- The neural networks were able to capture the underlying behavior of the experimental data, fitting to the overall shape of the TNM-B1 flow curves rather than the unwanted noise and variations between tests.
- Developing and computing the neural networks was completed in a timespan of minutes, potentially significantly faster than developing and computing a corresponding traditional model based on the same amount of experimental data.
- For the HIPed material state, good correlation was shown between the strain rate sensitivity maps, processing maps and optimal processing conditions based on the experimental and predicted data. For the heat treated state, a significant difference was observed in both the maps and the optimal processing conditions. This was likely due to the predicted flow stress for the HIPed state more closely matching the experimental data than the predicted stress for the heat treated state.

REFERENCES

Anderson, J.A., 1995, *An Introduction to Neural Networks*, A Bradford Book, The MIT Press.

Bambach, M., Sizova, I., Bolz, S. et al., 2016, Devising Strain Hardening Models Using Kocks–Mecking Plots—A Comparison of Model Development for Titanium Aluminides and Case Hardening Steel, *Metals*, 6, 204.

Cheng, L., Xue, X., Tang, B. et al., 2014, Flow characteristics and constitutive modeling for elevated temperature deformation of a high Nb containing TiAl alloy, *Intermetallics*, 49, 23–28.

Cingara, A., McQueen, H.J., 1992, New formula for calculating flow curves from high temperature constitutive data for 300 austenitic steels, *Journal of Materials Processing Technology*, 36, 31–42.

Inui, H., Kishida, K., Misak, M. et al., 1995, Temperature dependence of yield stress, tensile elongation and deformation structures in polysynthetically twinned crystals of Ti-Al, *Philosophical Magazine A*, 72, 1609-1631.

Levenberg, K., 1944, A Method for the solution of certain non-linear problems in least squares, *Quarterly of Applied Mathematics*, 2, 164-168.

Lin, Y.C., Zhang, J., Zhong, J., 2008, Application of neural networks to predict the elevated temperature flow behavior of a low alloy steel, *Computational Materials Science*, 43, 752-758.

Liu, B., Liu, Y., Qiu, C. et al., 2015, Design of low-cost titanium aluminide intermetallics, *Journal of Alloys and Compounds*, 650, 298-304.

Liu, Y., Zhao, T., Ju, W. et al., 2017, Materials discovery and design using machine learning, Computational Materials Science, 3, 159-177.

Marquardt, D., 1963, An algorithm for least-squares estimation of nonlinear parameters, *SIAM Journal on Applied Mathematics*, 11, 431–441.

Masahashi, N., Mizuhara, Y., Matsuo, M. et al., 1991, High temperature behavior of titanium-aluminide based gamma plus beta microduplex alloy, *ISIJ International*, 31, 728-737.

Pilania, G., Wang, C., Jiang, X. et al., 2013, Accelerating materials property predictions using machine learning, *Scientific Reports*, 3.

Prasad, Y.V.R.K., Sasidhara, S., 1997, *Hot working guide: a compendium of processing maps*, ASM International, Materials Park.

Prasad, Y.V.R.K., Seshacharyulu, T., 1998, Processing maps for hot working of titanium alloys, 243, 82-88.

Rojas, R., 1996, *Neural Networks: A Systematic Introduction*, Springer.

Sheikh, H., Serajzadeh, S., 2008, Estimation of flow stress behavior of AA5083 using artificial neural networks with regard to dynamic strain ageing effect, *Journal of Materials Processing Technology*, 196, 115-119.

Schloffer, M., Iqbal, F., Gabrisch, H. et al., 2012, Microstructure development and hardness of a powder metallurgical multi phase γ-TiAl based alloy, *Intermetallics*, 22, 231-240.

Yu, W., Li, M.Q., Luo, J. et al., 2010, Prediction of the mechanical properties of the post-forged Ti–6Al–4V alloy using fuzzy neural network, *Materials & Design*, 31, 3282-3288.

Zhu, Q., Abbod, M.F., Talamantes-Silva, J., Sellars, C.M. et al., 2003, Hybrid modelling of aluminium–magnesium alloys during thermomechanical processing in terms of physically-based, neuro-fuzzy and finite element models, *Acta Materialia*, 51, 5051-5062.

ZASTOSOWANIE SZTUCZNYCH SIECI NEURONOWYCH DO PRZEWIDYWANIA KRZYWYCH PŁYNIĘCIA I MAP PROCESÓW DLA TNM-B1

Streszczenie

Możliwość przewidywania zachowania się materiału jest istotna zarówno w badaniach naukowych jak i w inżynierii. Tradycyjnie to zadanie jest realizowane za pomocą modeli matematycznych na bazie opisu zjawisk fizycznych. Z drugiej strony, zachowanie się materiału jest zależne od szerokiego zakresu wzajemnie zależnych zjawisk, własności i warunków. W procesach odkształcania umocnienie, mięknięcie, rozwój mikrostruktury I generowanie ciepła występują równocześnie I mogą albo współdziałać albo konkurować ze sobą. Ponadto te zjawiska sa zależne od temperatury, przyłożonych sił i prędkości procesu. Ponieważ pełny opis zachowania materiałów w skalach od makro do atomowej nie jest jeszcze w pełni zrozumiały, takie procesy odkształcania jak na przykład kucie są trudne do opisamia przez modele fizyczne. Modelowanie odkształcania w wysokich temperaturach sprowadza się zwykle do wyboru punktów charakterystycznych z doświadczalnych krzywych płynięcia i wykorzystaniu ich do analizy regresyjnej. Takie modelowanie jest bardziej fenomenologicznym niż opartym na podstawowej teorii. Alternatywą jest wykorzystanie danych z doświadczenia do analizy danych lub uczenia maszynowego (ang. machoine learning - ML) w celu modelowania zachowania się materiału. Ponieważ model ML może uczyć funkcje mapujące łączące wejście z wyjściem tylko na podstawie danych doświadczalnych, wymaga on znajomości zjawisk fizycznych odpowiedzialnych za proces odkształcenia. W niniejszej pracy wykorzystano uczenie maszynowe do modelowania krzywych płynięcia aluminidku tytanu (TiAl) TNM-B1 w dwóch różnych stanach: ściskania izostatycznego na gorąco (ang. hot isostatic pressure - HIP) i po obróbki cieplnej. Sztuczna sieć neuronowa została zastosowana do uczenia funkcji mapującej, która przewidywała naprężenie uplastyczniające w zależności od temperatury, odkształcenia i prędkości odkształcenia. Dodatkowo sporządzono i porównano mapy wrażliwości na prędkość odkształcenia i mapy procesu bazuhące na danych doświadczalnych i obliczonych. Uzyskane wyniki wykazały, że sztuczne sieci neuronowe dostarczją realistycznych i dokładnych krzywych płynięcia, które odzwierciedlają wyniki doświadczeń eliminując szumy. Mapy wrażliwości na prędkość odkształcenia wykazały rozbieżne wyniki. Dobrą korelację między mapami obliczonymi i wyznaczonymi z doświadczenia zaobserwowano dla materiału w stanie HIP. Przeciwnie, duże rozbieżności wystąpiły w przypadku map dla materiału po obróbce cieplnej.

Received: November 10, 2018.
Received in a revised form: April 10, 2019
Accepted: April 11, 2019